JJEE
Volume 10 | Number 3 | September 2024 | Pages 397-414

Jordan Journal of Electrical Engineering

ISSN (print): 2409-9600, ISSN (online): 2409-9619

Homepage: jjee.ttu.edu.jo

Computer Vision-Based Method for Digitizing the Surface of the Dial Instrument and Tracking the Pointer's Movement

Mohammad Alfraheed[1, 2]

[1] Department of Computer Science, Faculty of Communications and Information Technology, Tafila Technical University, Tafila, Jordan
Email: Alfraheed@ttu.edu.jo

[2] Department of Computer and Information Science, College of Engineering and Computer Science, University of Michigan – Dearborn, Michigan, USA

Received: Nov 16, 2023 *Revised: Jan 05, 2024* *Accepted: Jan 10, 2024* *Available online: Jun 23, 2024*

***Abstract*—** Using the dial instrument for reading the oxygen pressure in the medical environment demands monitoring the pointer's movement and keeping track of its readings. Usually, the monitoring task is done by the administrator in the medical facilities. To ensure real time and accurate monitoring, the administrator must be supported by vision-based advanced methods to digitize the surface of the dial instrument and to track the pointer's movement. In this paper, a method is proposed to localize the three main references in the dial instrument, namely Pointer, FULL indicator, and EMPTY indicator. Once these references have been precisely determined, the proposed method records the status of the dial instrument. An emergency alert must be triggered while the pointer is moved toward the EMPTY area. Different computer vision techniques have been developed to implement the digitizing and monitoring in terms of real time constraint. The proposed method has been experimentally verified over 750 frames while the dial instrument was run and monitored the oxygen pressure. The obtained result unveil that the average running time is 0.316 s. The detection accuracy of the proposed method for these reference indicators varied from 88.5% to 100% over the first 30 frames of the tested video streams. Since the proposed method has been developed to keep track for the pointer's movement, it can recover the detection failure while dial instrument is running. Moreover, the proposed method can overcome the reading error of the pointer's centre point compared to the Hough transform method. Compared with the development of the Hough transform, the proposed method distinguishes itself by successfully employing morphological operations and color space processing to highlight region of interest, regardless of its high intensity values. In context of the applications of the pointer extraction of the dial instrument, another comparison has been conducted for the proposed method. The latter distinguished itself by digitizing the surface of the dial instrument without using the neural network mechanism; offering a recovery of the failure detection, and employing the idea of the black-white mask to concentrate the proposed method's developments.

***Keywords*—** Dial instrument; Pointer tracking; Computer vision.

1. INTRODUCTION

Recently, digital instruments are widely used due to their high precision, especially in medical purposes [1]. The instrument dial is still used in most of the hospitals. Despite the instrument dial has a communication interface, it is important to record the instrument readings in terms of the medical applications. The recording must be implemented automatically not only to reduce the error of manual reading, but also to improves the accuracy of the information. In some situations (i.e., hospitals), such communication interface is not unfortunately available. The instrument readings must be then recorded manually. In this paper, the advanced techniques of computer vision have been applied to recognize the instrument dial. The recognized data identified by the proposed method can be transmitted to

* Corresponding author
DOI: https://doi.org/10.5455/jjee.204-1700170952

the control centre. The latter can realize the real data to meet the necessary requirements of the standard supervision and real environment.

The dial instrument used in this paper is shown in the Fig. 1. In such dial instrument, the pointer is moved in direction from FULL position to EMPTY position or in opposite direction. The pointer can be rotated by 0° – 90°. The proposed method is thus required to recognize three reference points: position of pointer, position of the FULL indicator and position of the EMPTY indicator. Extracting area of interest from the circle area of the dial instrument is first necessary to highlight these reference points. Once the pointer of the dial instrument is detected, both other reference points are recognized based on their deviation angle from the center of the pointer. However, the interface of the instrument dial is sometimes complicated because its glass surface usually generates reflection. This reflection will change the colour appearance of the instrument dial. These factors will make it difficult to segment the reference points of the instrument dial. In this paper, a computer vision-based method has been proposed to overcome these challenges and to successfully extract area of interest.

Fig. 1. The dial instrument utilized in this article.

The rest of this paper is organized as follows: in section 2, the related work has been discussed. The proposed method has been addressed and discussed in the third section. The results and discussion have been highlighted in the fifth section. Finally, the conclusion has been given in the last section.

2. RELATED WORK

Solving the position problem for object of interest plays an important role in many of application-based on the reading area position. In [1], three main existing positioning methods have been discussed which are texture analysis, Edge detection and color space analysis. Tao Wang et al [1] have proposed a method for digital reading positioning using color characteristics. Although the color characteristics suffer from less efficiency in complicated background environment, it can be considered as a starting step to find more information about color distribution in the application environment. Extracting features of interest is then developed to overcome thresholding problems of edge detection. Another automatic identification system has been proposed in [2] for automatic identification of digital ammeter and digital voltmeter. They have used RGB features to get grayscale images and the weight distribution has been used to extract digital number from the environment backgrounds. Unfortunately, the digital number in LCD screen does not suffer from color distribution and background problems as it is in pointer instrument systems. Cui Wang et al [3] have proposed

a dial printing system for pointer instrument. Their proposed system highlighted two image edge detection based on canny detector and Hough transform to recognize the straight lines of the pointer. They depended on the LED light to reduce the noise ratio and background complexity. LED light has a lot of advantages, but it is not available in many traditional and real environments. Another similar research [4] has been proposed to ammeter recognition using Wearable device which increase the running cost of the prosed solution. Considering the lows cost has been highlighted in [5] by kai Cheng et al. In both [4, 5], they have employed Hough transform and other image processing functions to detect the pointer in the mechanical pointer instrument panel. They assumed the dial instrument is in the solid background and there are no environmental effects surrounding the instalment dial. The classical Hough transform has been improved in [6] by fixing the centre of the dial instrument. The characteristics of the instrument image has been considered to extract the dial pointer from the surrounding environment. They have applied a complicated process to read the dial pointer without paying attention to the other important indicators in the dial instrument (i.e., Empty indicator). The pointer position of the instrument dial has been considered in [7] by designing an embedded image recognition system. The center projection method and template matching method have been used to grantee extract the position and the instrument dial. Within their system, preprocess parameters must be offered to successfully run their system. These parameters must be recalibrated once the environment is changed, or the system is shifted. Another proposed reading system has been developed in [8] for a water meter instrument. Their system has been designed inside a lab, in which images are captured. The dynamic and complicated environment are then not tested. A simulated change and complicated environment have been offered in [9]. Their proposed method has an assumption where the instrument is tilted by a certain degree to right or left. Normally, the dial instrument is fixed, and the pointer is not affected in case of the tilt of dial. In [10], several of the complicated environmental problems have been addressed. Some of these problems are influence of uneven illumination, complex background, rotation angle, image blur, shooting angle. Even though they have proposed a method to overcome these problems using convolutional neural network, the traditional techniques of computer vision are able to solve these problems smoothly. The accuracy of instrument recognition can be improved by enhancing the recognition parameters which are extracted from the dial instrument itself. Using the convolutional neural network requires more complex time and memory. Another research has been introduced in [11]. They combine the traditional dial extraction algorithm with deep learning algorithm. Despite their work having improved the traditional method of dial instrument extraction, it had consideration to detect the dial instrument and its pointer without paying more attention to other details of the dial instrument surface.

As a summary, the references mentioned in the related work have been varied from 2018 to 2023. Using advanced techniques, for example, convolution neural networks and deep learning algorithm, has been considered in both recent works [10, 11] to recognize the dial instrument. However, both works must consume time and memory resources. The proposed method here has developed the traditional tools in computer vision to detect and extract the surface of the dial instrument without using a huge time and memory resources.

The detection concept has been introduced by [12] in cooperation with the generalize Hough transform algorithm (called HoughNet). Their method has been developed to determine the object's location using a sum of votes which refer to the object of interest. Their

detection model has been developed based on testing the input image over single scale and multi-scale resolutions. The effectiveness of HoughNet is that their work has been developed without using the advanced techniques of the neural network for saving the available resources. Moreover, the Hough transform is being developed in much research to improve the objects detection accuracy. Inspired by the HoughNet, the work has been discussed to use the traditional techniques of computer vision for detecting and tracking the main references of the dial instrument in terms of saving the available resources. Increasing the detection accuracy of the Hough transform has been also discussed [13] using the information obtained from other sensors sources (i.e. radar sensors). Their work has also been considered as other efforts for improving the Hough transform techniques without using neural network concepts. In [14], the Hough transform has been used for detecting and recognizing objects of interest. morphological operations have been combined with the Hough transform to increase the detection accuracy. The last recent three references discussed above introduced evidence 4in which researcher have been developing the detection using traditional Hough transform with computer-vision techniques to detect the object of interest. The comparison between these methods and the proposed method has been suspended to the section of the result in this article.

Furthermore, the traditional techniques of computer vision have been improved by extracting reference points of dial instrument surface (i.e. FULL and EMPTY area) not only to increase the detection accuracy of the pointer dial instrument, but also to fix these reference points for improving the digitizing process of the dial instrument.

3. THE PROPOSED METHOD

The key purpose of the proposed method is to improve the detection accuracy of the pointer dial instrument. Moreover, some of surface details of the dial instrument can be extracted. These details enable the proposed to digitalize the pointer movements. Before extracting the inside details of the dial instrument, its circle position is given, and the pointer is initially detected. This task has been offered before as an initial process. In the following sub-sections, the steps of the proposed method have been implemented:

3.1. The Histogram Processing Based on the Color Space HSV

Processing a color space of the image of interested is a necessary step in many detection applications[15, 16] due to the need to remove the noise pixels, appearance enhancement and improving the detection accuracy. The main aim of this step is to improve the appearance and to highlight the reference points on the surface of dial instrument. Furthermore, the light reflection generated by camera light is consequently eliminated. Many color spaces have been compared with each other in this step for the captured frame of the dial instrument.

Fig. 2a to Fig. 2d show the comparison between these color space which RGB, HSV, YCbCr and L*a*b respectively. The comparison shows the HSV can highlight, better than others, the reference points of the dial instrument which are FULL indicator, EMPTY indicator, and the dial Pointer. In more details, the color space HSV has been shown in Fig. 2a. The color space of histogram is shown in Fig. 2a, in which the histogram has not changed or processed. Highlighting the reference points has been manually generated for the captured frame. The reference points have been marked by a black color more than other surrounding points.

Although the histogram process has been manually implemented, it can be automatically run for other frames. Fig. 2b process shows the highlighted reference points, and the new shape of histogram is also shown in the right side after it has been processed.

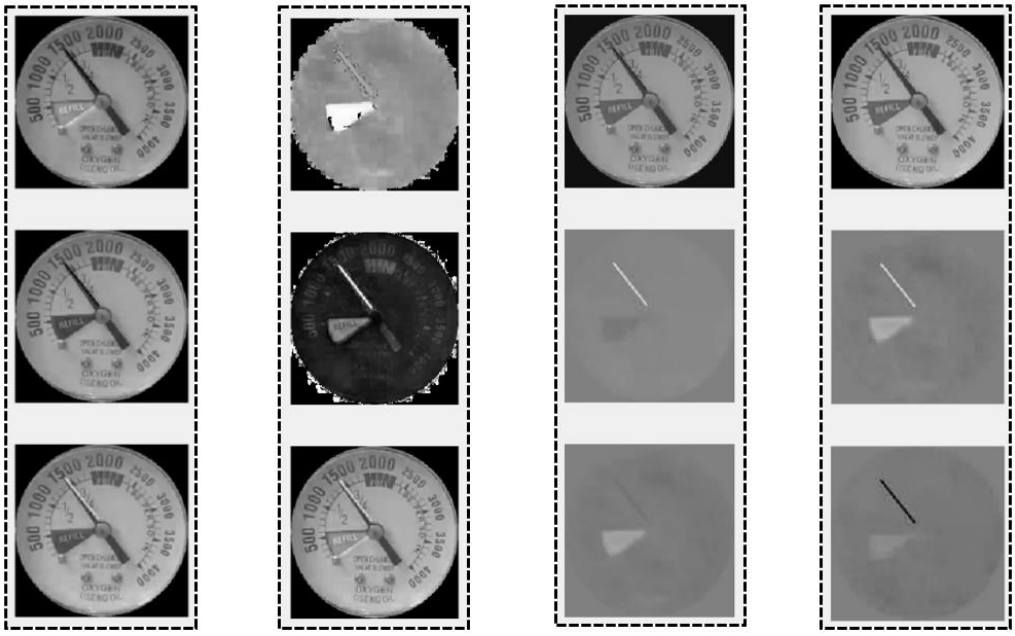

Fig. 2. Four color spaces for the dial instrument: a) RGB; b) HSV; c) YCbCr; d) Lab.

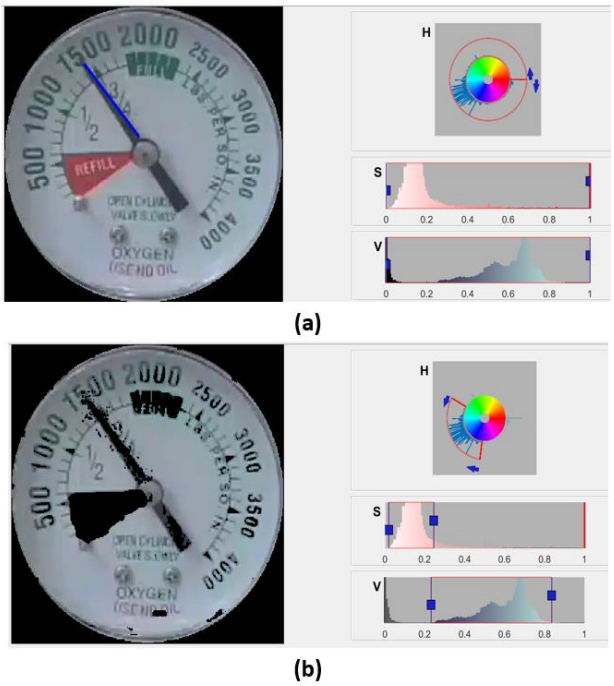

Fig. 3. Histogram shapes of the color space HSV for the dial instrument: a) before processing; b) after processing.

As a result, a mask is generated for the captured frame, and it is used for the next frames. The mask has been shown in Fig. 3b at the left side. The mask was generated by focusing on the interested values over the S-Band or V-Band of the HSV- color space. Adjusting the blue vertical lines shown in Fig. 3 has been manually implemented and these interested values were highlighted. In the corresponding mask, these values were replaced by a zero value and were coloured by Black. Applying the generated mask over the captured frame will generate the

Black-White image which shows the region of interest without the need to apply morphological operation. That is the reason behind using the adaptive color-space processing. The consumed time is then reduced beside the memory cost.

3.2. Extracting the Connected Regions of Interest

Analyzing the BW image generated from the previous step is a necessary operation due to the need to convert the image into a symbolic image [17]. The symbolic image includes then the connected components which are marked by a unique number. The idea behind extracting the connected components here is to optimize the runtime and memory consuming. Instead of processing the whole frame, the region of interest is extracted and considered. Several methods of finding the connected components have been developed in the last 5 years [18]. Here, the 4-connectivity [19] has been employed to process the BW image and extract the connected regions. The 4-connectivity depends on the rule of two adjoining pixels in which the method is looking for the connected pixels along the horizontal and vertical direction [19]. Fig. 4 shows the centre of the connected components.

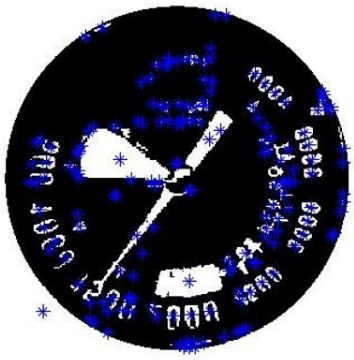

Fig. 4. The centre of the connected area is in the Black-White frame of the dial instrument.

3.3. Extracting the Surface of the Dial Instrument from the Complicated Environment

As shown in the previous step, the complicated environment means that there are many regions located around the reference points. Some of these regions are located on the surface of the dial instrument and others are positioned outside of the circle shape of the dial instrument. These scattered regions (non-interested connected area and interested connected area) are normally generated due to the light reflection, instrument glass reflection, camera shadow or low resolution of the camera. The interested connected area must be distinguished from those non-interested. Both types of connected regions were located on the surface of the dial instrument. The reason behind excluding the non-interested regions is to focus the development and processing given by the proposed method on what its need. Since those non-interested connected area does not play any role within this work, they were excluded. The solution proposed here is to extract the surface of dial instrument based on the pointer position. The surface is shaped as a circle in which its centre is the centre of dial instrument (CN), and the radius is the pointer length of the dial instrument (L). The CN is positioned in 2D-coordinates by CNX and CNY. Both CN and L are given as an input for the proposed method. Using both parameters CN and L an internal circle has been located as shown in Fig. 5a. Four parameters must be calculated to locate the horizontal and vertical border for the dial instrument. these parameters are MIN_Y (which is the minimum y-coordinates), MAX_Y (which is the maximum y-coordinates), MIN_X (which is the minimum x-coordinates), and

MAX_X (which is the maximum x-coordinates). They are calculated based on the following equations:

$$MIN\_Y = CN_Y - L \quad (1)$$

$$MAX\_Y = CN_Y + L \quad (2)$$

$$MIN\_X = CN_X - L \quad (3)$$

$$MAX\_X = CN_X + L \quad (4)$$

Beside of these parameters shown in Fig. 5a, the centre of the connected scattered area (C) is calculated based on the following equations:

$$C = (Cx, Cy) \quad (5)$$

$$Cx = (X1+X2+X3 + \ldots\ldots + Xn) / N \quad (6)$$

$$Cy = (Y1+Y2+Y3+ \ldots\ldots + Yn) / N \quad (7)$$

where:

C: It is the center point of the connected area.

Cx: the average of the x-coordinates of points associated with the connected area.

Cy: the average of the y-coordinates of points associated with the connected area.

Xi: the x-coordinates of points associated with the connected area.

Yi: the y-coordinates of points associated with the connected area.

N: the number of the pixel points in the connected area

Since the number of the connected scattered regions are greater than the required reference points (i.e. FULL, EMPTY and Pointer), a filter has been applied to ignore the non-interested connected area Fig. 5b. The number of the pixel points of the connected area (i.e. N) has been used as an input for the filter which is run based on the following function:

$$f(N) = \begin{cases} Non - Interested\ Area, & N < TN \\ Interested\ Area, & N \geq TN \end{cases} \quad (8)$$

where: TN: It is the target number of points given by the user.

Fig. 5c shows results generated by extracting and locating the surface of the dial instrument. Many of the interesting area have been located. The regions of the dial surface have been highlighted by the yellow color. Some of these interested areas have been located despite they are not used as reference points, which are shown in Fig. 5c marked by red line.

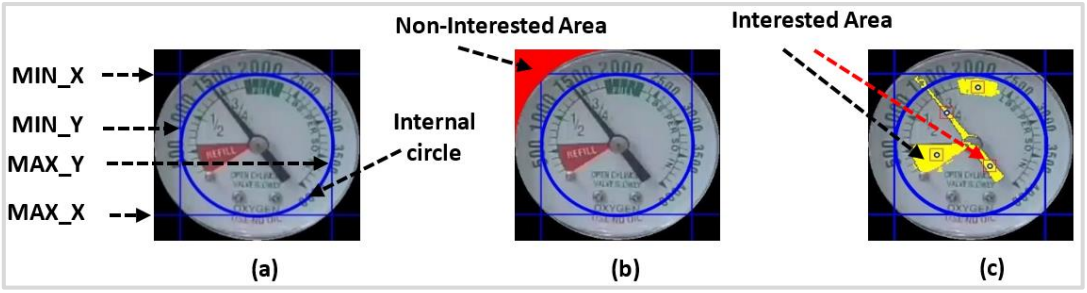

Fig. 5. The results generated from extracting the surface of the dial instrument: a) four parameters; MAX_X, MIN_X, MAX_Y, MIN_X and the internal circle of the dial instrument; b) marking the red area as non-interested area due to locating it out of the four parameters coordinates; c) marking the interested area by yellow color.

3.4 Accurately Detecting the Pointer's Position on the Surface of a Dial Instrument

The initial location of the pointer in the dial instrument has been given to the proposed method. However, it does not sometimes intersect with the detect interest area either due to illumination reflection or complex background. These external effects have been addressed in [10]. The need of precise detection of the pointer is therefore addressed in the proposed

method. Furthermore, it is so necessary to successfully fix a strong reference point in the surface to be used later for precisely highlighting other reference points (i.e., FULL, EMPTY indicators) in one hand. In other hand, the proposed method can be digitalized the pointer's movement instead of using the digits drawn on the surface of the dial instrument. Instead of using neural network algorithms to remove such effects [10], traditional computer vision techniques can be developed to precisely detect and locate the pointer's position. These techniques save more effort in terms of time and memory complexity.

The solution proposed here is to locate a horizontal line for each a detected connected area. The line must pass through the centre point of the connected area. These horizontal lines have been located based on the following equation [20]:

$$\text{LineCN}=mX+b \tag{9}$$

where:

LineCN: is the horizontal line passing through the center of the connected area.

m: is the slope of the line.

b: is the constant value.

X: is the x-coordinates points locating on the right and left side of the centre point.

Another line must also be located for the initial pointer given as an input for the proposed method. The pointer line is located using the CN (CNX, CNY) and the Pointer length (L). Fig. 6 shows the pointer line colored by blue. The pointer line has been located based on the following equations [20]:

$$LinePT_X = CN_X + L * \cos(\theta) \tag{10}$$

$$LinePT_Y = CN_Y + L * \sin(\theta) \tag{11}$$

where

$LinePT_X$: is the x-coordinate of the end point of the pointer line.

$LinePT_Y$: is the y-coordinate of the end point of the pointer line.

CN_Y : is the y-coordinate of the center point of the dial instrument.

CN_X : is the x-coordinate of the centre point of the dial instrument.

L: is the pointer length of the dial instrument.

θ: is the slop angle of the pointer.

The idea behind precisely detection of the pointer area is to find the intersection between $LinePT$ and $LineCN$. Once the intersection is generated, the detected connected area is marked as main reference point in the dial instrument. Finding the intersection is figured out based on the several steps. First, the start point (x_1, y_1) and end point (x_2, y_2) for $LineCN$ are generated. Second, the start point (x_3, y_3) and end point (x_4, y_4) for $LinePT$ are calculated. Third, the intersection point has been calculated based on following equations [21]:

$$\alpha = \frac{((x_1-x_3)*(y_1-y_2)-(y_1-y_3)*(x_1-x_2))}{((x_1-x_2)*(y_3-y_4)-(y_1-y_2)*(x_3-x_4))} \tag{12}$$

$$\beta = \frac{((x_1-x_3)*(y_3-y_4)-(y_1-y_3)*(x_3-x_4))}{((x_1-x_2)*(y_3-y_4)-(y_1-y_2)*(x_3-x_4))} \tag{13}$$

$$f(\alpha,\beta) = \begin{cases} Intersection\_Exist, & \alpha \in [0,1] and\ \beta \in [0,1] \\ NULL, & \alpha \notin [0,1]\ or\ \beta \notin [0,1] \end{cases} \tag{14}$$

After calculating the parameters α and , the intersection is detected based on the values of both parameters. If both values are greater than zero and less than 1, the intersection is highlighted. Fig. 6 shows $LineCN$ for each connected area and the intersection between both $LinePT$ and $LineCN$.

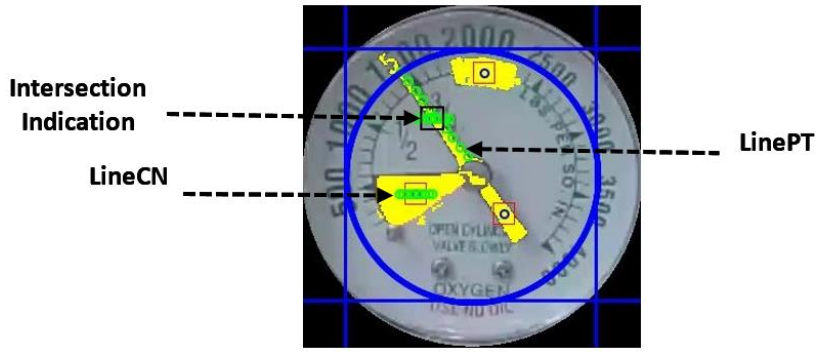

Fig. 6. Illustration based on the dial instrument for finding intersection.

3.5 Detecting the Main Reference Points of the Dial Instrument

After emphasizing the location of the pointer in the dial instrument, the need to locate other reference points is given the next priority. The FULL and EMPTY area must be precisely defined not only to highlight the details of the dial instrument but also to digitalize the pointer's moves. It is so necessary to clarify the oxygen pressure and what is the current situation of the medical system. Since the initial location of these reference points have been given from the previous step, the contribution here is to distinguish these reference points from other surroundings connected area. Some of recent researches have employed the neural network algorithm and other artificial intelligence tool to classify the surface of the dial instrument and to locate the reference points [4, 10]. Despite the neural network grants an advanced solution, it increases the costs of the proposed method in context of time and memory complexity. The solution proposed here to detect other main references depends on finding the deviation angle of the connected area. As for FULL and EMPTY area, their centre points are always located on the right side and left side of the pointer respectively. Fig. 6 shows the centre of each connected area marked by a circle and rectangle. The angle must be shaped from three points which are as follows:

- PointA is the intersection point of the pointer as shown in Fig. 7. PointA consists of 2D-coordinates $PointA_X$ and $PointA_Y$.
- PointC is located on the pointer towards the centre of the dial instrument. PointC consists of 2D-coordinates $PointC_X$ and $PointC_Y$.
- PointB is the center of the connected area. It consists of 2D-coordinates $PointB_X$ and $PointB_Y$.

Both PointA and PointC are fixed, while the PointB is changed for each connected area. Therefore, two vector line are generated. The first is between the PointA and PointB, whereas the second line is between PointA and PointC. Each of these vector lines is calculated in both x-coordinates and y-coordinates. Respectively, the length of each vector is calculated in both coordinates using the following equations [22]:

$$LengthAB_x = |PointA_x - PointB_x| \quad (15)$$

$$LengthAB_y = |PointA_y - PointB_y| \quad (16)$$

$$LengthAC_x = |PointA_x - PointC_x| \quad (17)$$

$$LengthAC_y = |PointA_y - PointC_y| \quad (18)$$

The deviation degree $DevAng$ has been calculated based on the following equation [23]:

$$DevAng = atan2(\left[LengthAB_x * LengthAC_y - LengthAC_x * LengthAB_y\right], \left[LengthAB_x * LengthAB_y + LengthAC_x * LengthAC_y\right]) \quad (19)$$

where

$LengthAB_x$: The x-coordinates distance between the PointA and the PointB.

$LengthAB_y$: The y-coordinates distance between the PointA and the PointB.

$LengthAC_x$: The x-coordinates distance between the PointA and the PointC.

$LengthAC_y$: The y-coordinates distance between the PointA and the PointC.

$DevAng$: the deviation angle between the connected area A & B.

Once the $DevAng$ is greater than 1, it is considered as the main reference point. To distinguished which the point is FULL or EMPTY, the parameter $LengthAB_x$ is used. In case it is positive, the point is addressed as FULL Point and $DevAng$ has positive sign because the x-coordinate of PointB is greater than x-coordinates of PointA. Otherwise, the PointB is addressed as EMPTY Point and $DevAng$ has negative sign. If there are multi values of $DevAng$ (either positive or negative), the largest value is assigned as the target value. Fig. 7 shows the main parameters used in the equations above.

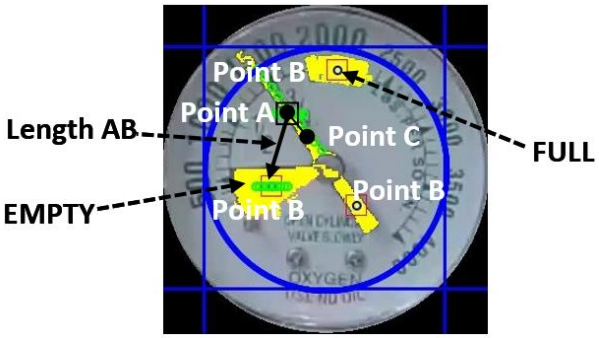

Fig. 7. The main parameters used to calculate the deviation degree.

4. RESULTS AND DISCUSSION

Here, the proposed method has been implemented using MATLAB. Tools for computer vision and image processing had been developed in the proposed method. The experiment and performance evaluation were carried on video frames captured for oxygen regulator installed in public hospitals of the Jordanian ministry of health.

The proposed method has been successfully run to detect the FULL and EMPTY Area in the instrument dial. Fig. 8 shows values of $DevAng$ used to find the position of both Areas. The proposed method has been running over a video file for over 2 minutes. The results shown in Fig. 8 has been generated from around 150 frames of the video file. The $DevAng$ has been explained as follows; Once the value is greater than 1, the centre point of the interested area has been located on above of the pointer. As shown in Fig. 8 the centre points of the FULL Area have been marked by red color. In contrast, the values $DevAng$ less than zero have been marked by blue color, which have associated with the EMPTY area. These blue values have been located under the pointer's center points. The latter has been marked by green color. Beside the location of both Area have been located based on the $DevAng$, the coordinate average of each Area can be identified because each area can be successfully separated. The circles located in Fig. 8 show that those coordinates can be gathered in groups which can generated many of statistical values (i.e., mean). The error of failure detection has been detected also from the scattered values shown in the Fig. 8.

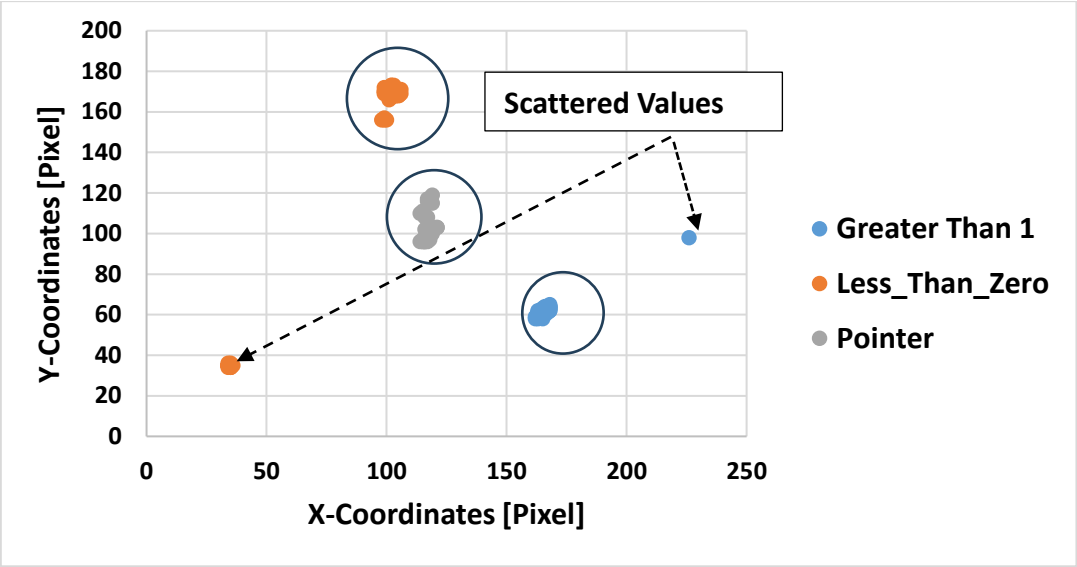

Fig. 8. The detection of the FULL and EMPTY AREA based on the parameter DevAng.

Another contribution of the proposed method is to precisely detect and track the pointer in the dial instrument. The Fig. 9 shows the centre point of the pointer in the dial instrument while the proposed method is run over 150 frames. The centre point of the pointer has been marked by red color in the tested frame.

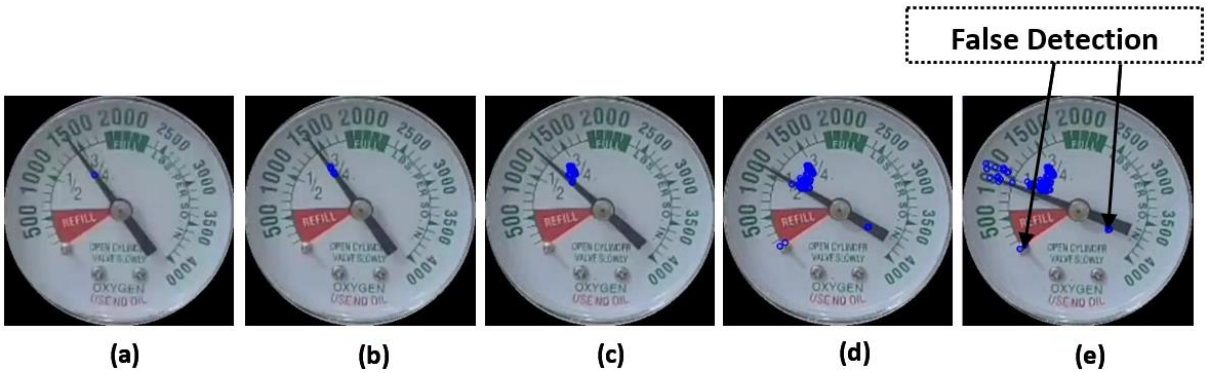

Fig. 9. The Results generated for detecting and tracking the centre point of the pointer over 150 frames from the frame numbered by: a) 1; b) 10; c) 50; d) 100; e) 150.

Furthermore, the proposed method has kept a record for the previous coordinates of the pointer in the previous frames. Keeping track of these centre points can enable the proposed method to overcome the false detection. The latter has been generated by detection another Area which is similar the pointer area as shown in Fig. 9. Once the proposed method cannot precisely the centre of the Pointer, the head point of the pointer has been determined as a reference point of the pointer. Therefore, some of these points have been marked by red circles which are close to the head of the pointer as shown in Fig. 9e.

Keeping a track of the pointer's move is necessary feature of the proposed method because the digitalization of the instrument dial can be generated instead of digit indications drawn in the instrument surface. Fig. 10 shows a yellow line for a track record which has been generated based on the first and the last value of the pointer's coordinates. In the Fig. 10, the track record has been shown for many cases which are for first 70 frames, 90 frames, 110 frames, 130 frames and 150 frames. These cases have been shown in Fig. 10a to Fig. 10e respectively.

In more detail, the first ten frames have been considered to show the coordinates of the pointer's move. Fig. 11 shows the x-coordinates and y-coordinates for the centre points of the

pointer while it was moving towards the EMPTY Area. Each centre pointer associated with the frame has been in the 2-dimensional histogram. The linear line (dot line) has been generated for confirming that the mean values of these values can be used to digitalize the pointer's move.

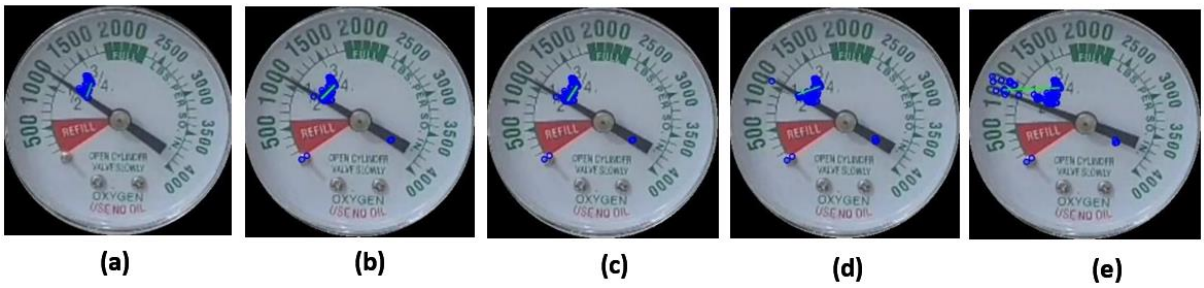

Fig. 10. The Track record drawn by yellow line for results generated by detecting and tracking the centre point of the pointer over 150 frames till frame numbered by: a) 70; b) 90; c) 110; d) 130; e) 150.

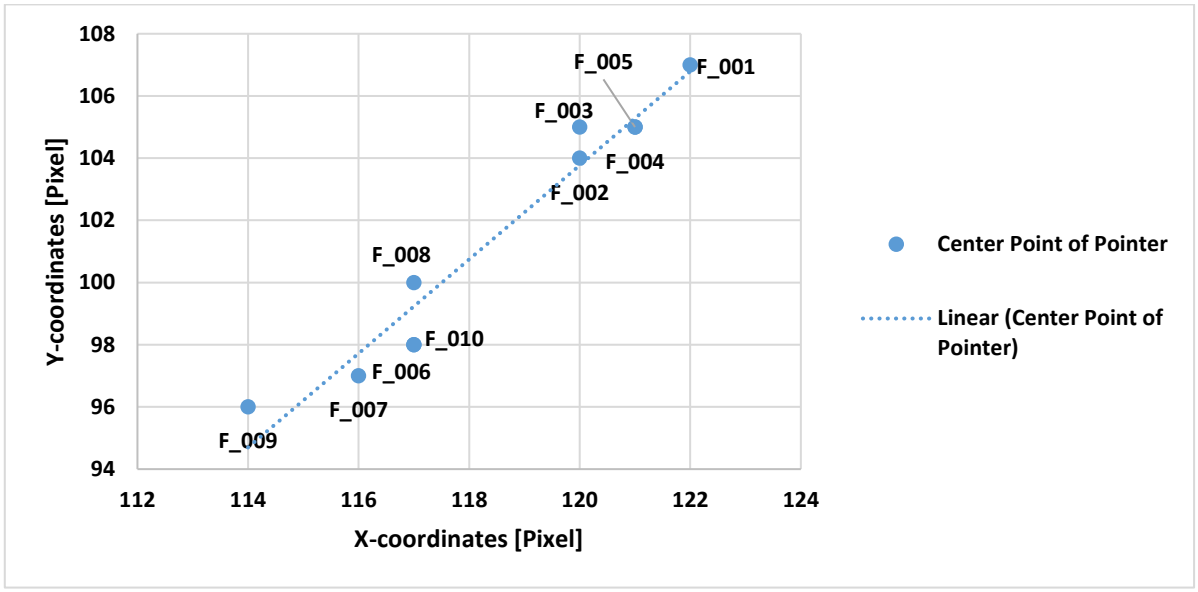

Fig. 11. X-coordinates and y-coordinates for centre point of the pointer in frames numbered from 1 to 10.

For more tested frames, Fig. 12 shows the linear line for frames from 1 to 148 increased by 10. Although there are some values scattered, the linear line can be used to estimate the previous and the next value of the coordinates of the pointer's centre point. Furthermore, the monitor process of the pointer's move can be given by generating such linear line. Once the next coordinates of the centre point are located away from the estimated value of the linear line, the proposed method can generate an alert for which the pointer's position has unexpected changed.

The proposed method has been tested over three video stream named Video#2, Video#3 and Video#4. A captured frames have been shown in Fig. a, 13b and 13g for these video streams respectively. Each video stream has approximately 200 frames. Although these videos stream look similar, they have different intensity variation. Each one has been manipulated by the HSV histogram processing mentioned above, which has been implemented by adjusting the minimum and maximum intensity values in each band of the color space HSV. Each video stream has a different image mask to generate the corresponding black-white image. These black-white images are not perfectly similar because the input video stream is different from each other. These black-white images or masked images have been shown in Fig. b, 13e and 13h for those video stream respectively. The three main reference points have been

consequently extracted as shown in the Fig. c, 13f and 13i for three video stream respectively. The pointer has been marked by a blue line and red rectangle. The Full point has been located by the green rectangle, where the EMPTY has been marked by the white rectangle. Since the reference point have been extracted over the first 27 frames, the generated results have been shown in the Fig. c at the frame numbered by 27 for the Video#2. In both video#3 and Video#3, the results have been extracted from the frame numbered by 30. Using around 30 frames for locating the FULL and EMPTY reference points was enough to fix successfully and precisely these points on the surface of the dial instrument while the pointer was still moving toward FULL or EMPTY point. Therefore, the proposed method needs approximately 1 s or less to locate these points. By the assumption that the frame rate of the video is 32 frames/s.

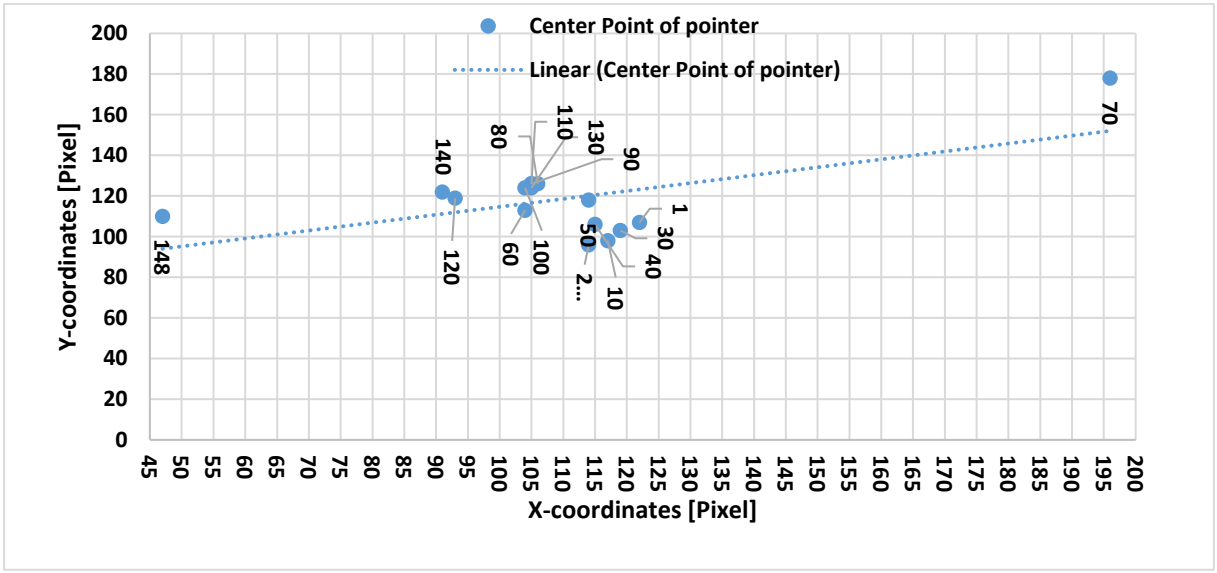

Fig. 12. X-coordinates and y-coordinates for the centre point of the pointer in frames numbered from 1 to 124 increased by 10.

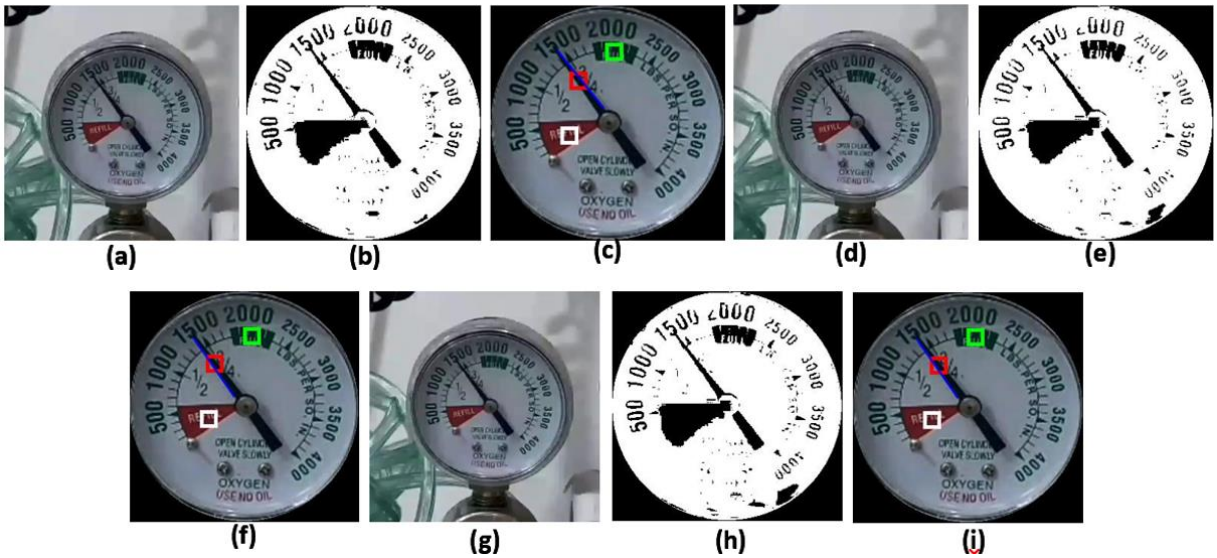

Fig. 13. The main recognized reference points (Pointer, FULL and EMPTY) generated for different videos: a) the captured frame of second video stream (Video#2) and its generated mask; b) and c) the extracted reference points of Video#2; d), e), and f) the captured frame of the third video stream (Video#3), its generated mask and the extracted reference points, respectively; g) and h) a sample of the fourth video stream (Video#4) and its generated mask, respectively; i) the extracted reference points of the Video#4.

Showing the results generated by the proposed method over the three video streams have been presented in the Fig. . The x-coordinates of the three main reference points have been used to show where these points have been located. Ignoring the y-coordinated was just due to the need to simplify the point's movement and the y-coordinates were still used to locate these points in the captured frames. Moreover, the x-coordinates of the reference points associated with the Video#3 have been multiplied by 2 times because they would be shifted up to separate each result for the video stream from other in the Fig. . For the same purpose, the x-coordinates of the reference points generated from the Video#4 have been multiped by 4 times. The first 30 frames from each videos stream have been used to track the x-coordinates of the reference points. 30 frames represent approximately the first second of the video stream. Locating these points within 1 s was enough to satisfy the real time constraints.

As shown in the Fig. , the x-coordinates of each reference point associated with the video stream Video#2 have been marked by the first three horizontal lines of the chart data. As long as the data points of the horizontal line for each reference point have been positioned adjacent to each other, the proposed method can estimate and fix the location of the reference point. Once the value of the x-coordinate has been changed up or down, the proposed method failed to locate the coordinates of the reference point over the input captured frame. However, the proposed method can not only detect the failure detection but also can estimate the correct position from the previous values of the coordinates of the reference point. The successful rates of the proposed method for the Video#2 are 96%, 76.9% and 88.5% respectively for the POINTER, FULL and EMPTY points.

Based on the results given from the Video#3, the successful rates of the proposed method are 100%, 96% and 96% respectively for the POINTER, FULL and EMPTY points. In contrast, the Video#4 has generated successful results for POINTER, FULL and EMPTY points which are 100%, 88.5% and 96% respectively. Notably, the proposed method can eliminate the failure detection for those reference points through estimating the correct position from the generated history values.

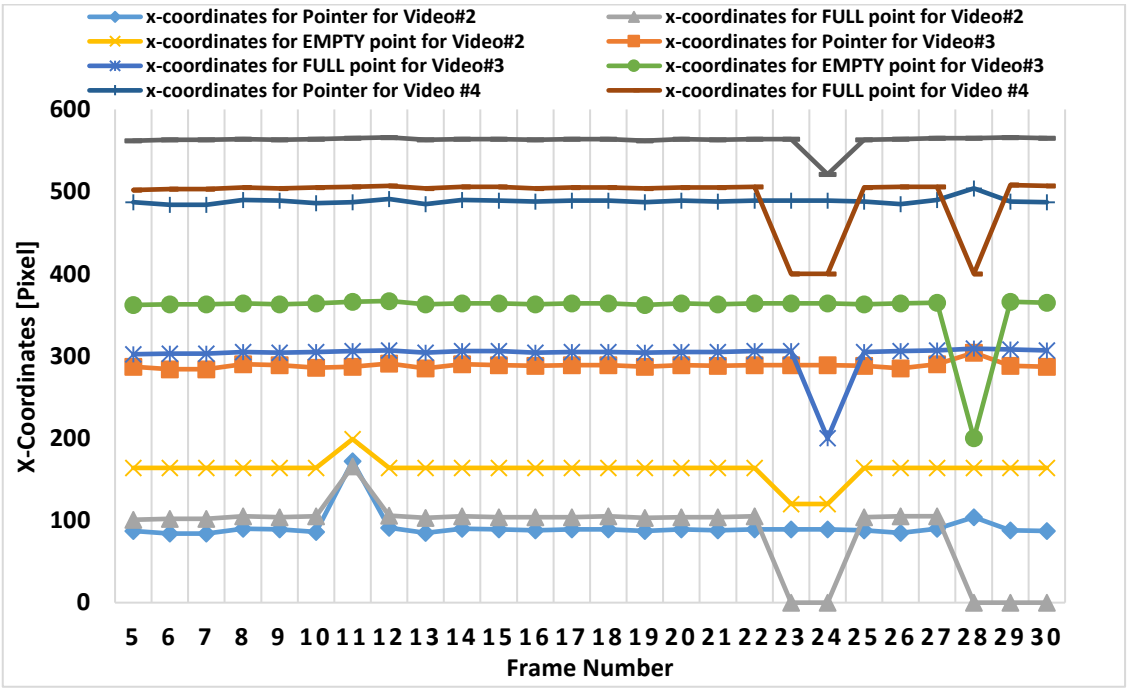

Fig. 14. X-coordinates of reference points (Pointer, FULL and EMPTY) over the first 30 frames of Video#2, Video#3 and Video#4.

The results of the proposed method have been compared with the Hough transform method [14]. Fig. shows the comparison based on different cases. First case has been shown in Fig. a, and 15b. The false detection generated from the Hough transform method for line detection has been shown in Fig. a. The proposed method has improved the results by successfully detecting the pointer. The second case has been shown in Fig. c and 15d. In this case, the false detection (shown in Fig. c) can be improved by finding the alternative detection shown in Fig. d and marked by white color. Both Fig. e and 15f represent the third case, where the false detection can be improved by a track of the pointer's move. Although there is no alternative detection for the pointer due to the small size of the marked area of the pointer, the proposed method can be able to estimate the next coordinates of the pointer. The last case has been given in the last two figures, i.e., Fig. g and 15h. because the pointer has been moved toward the EMPTY area, the marked area has been merged with each other. Once the distance between the pointer's centre point and the EMPTY area closes to zero, the proposed method has been developed so that there is no need to detect the pointer's move. Priority has been given to declare an emergency alert for monitoring the oxygen pressure.

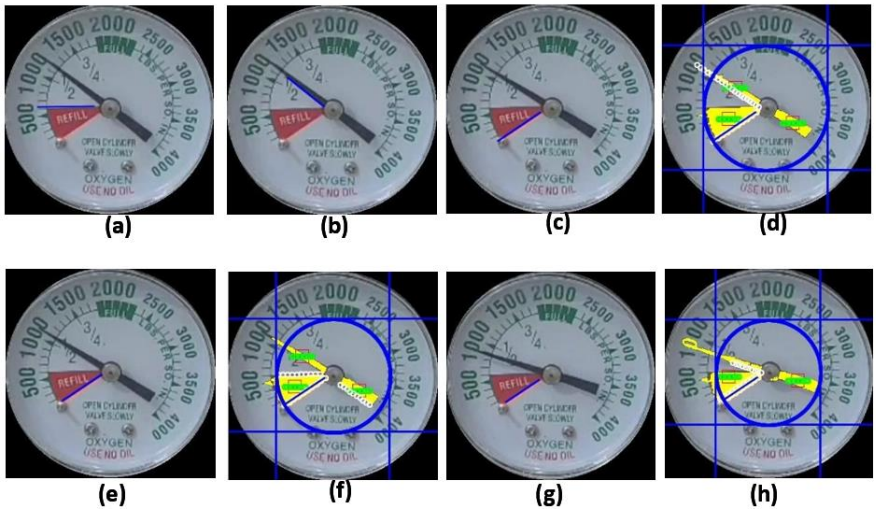

Fig. 15. A comparison based on the results of the proposed methods and the Hough transform method for different cases: a) and b) the first case; c) and d) the second case; e) and f) the third case; g), h) the fourth case.

A comparison has been conducted between the proposed method and other methods related to the Hough transform developments is shown in Table 1.

Table 1. Comparison between the proposed method and other methods in context of the Hough transform developments.

Method	Parameter		
	Using morphological operations	Depending on the high intensity	Testing in an applied application
HoughNet [12]	No	Yes	Yes
Modified Hough Transform Method [13]	No	No	Yes
Applied Hough transform [14]	Yes	Yes	No
The proposed method	Yes	No	Yes

These methods were discussed above, which are HoughNet [12], Modified Hough transform Method [13], Applied Hough transform [14]. The shared concept between these discussed methods is to develop the Hough transform method for improving the accuracy of

object detection. Three parameters have been used. The first parameter is about using morphological operations. The idea behind using the first parameter has been arisen from the effects of the morphological operations in focusing the developments on the region of interest and saving the running and memory resources. The second parameter is titled by Depending on the High Intensity. Despite the method saves efforts and highlights the region of interest from surroundings, many objects of interests have been fused in dynamic environments and they have not a high intensity to be distinguished. The third parameter is called Testing in an applied application. Since the performance of the developed method must be shown in context of real time constraints, the third parameter refers to whether the method has been tested against real problem developed in an application.

As a summary for the proposed method concerning of the object detection in terms of Hough transform method. The method distinguished itself from other methods by using the morphological operations in cooperation with the histogram color space processing. Using both morphological operation and color space processing enables not only to focus the proposed method's operations on the regions of interest but also to highlight these regions even though they have not a high intensity values and they have a variation intensity. Testing the proposed method has been implemented for applied application which need real time constraints to be run. Other compared methods have been suffered from fused these parameters in their developments, despite of their good results. Moreover, the method introduced in [14] has achieved good results but they have functioned a classification function likes neural network. The latter costs more efforts in development in terms of time and memory constraints.

Another comparison has been conducted with other methods which have used their developed methods for extracting the pointers from the dial instruments as shown in Table 2.

Table 2. Comparison between the proposed method and other methods in context of pointer extraction from the dial instruments.

Method	Parameter		
	Using neural network	Recovery of failure detection	Using mask for dial instrument
Method with deep learning [11]	Yes	No	Yes
Intelligent recognition [10]	Yes	No	No
The proposed method	No	Yes	Yes

The comparison has shown how the proposed method distinguished itself from other by extracting and tracking the pointer located in the dial instrument. In addition, the latter has been digitized by positioning the main reference points FULL and EMPTY on the surface of the dial instrument. Three parameters have been used in the comparison. The first shows whether the method has been developed using the neural network algorithm. Whenever the method depends on the neural network algorithms, it must pay more efforts for advanced running and memory consuming. The second parameter is about the failure detection. Can the developed method recover the failure detection? The last parameter is to use the black-white mask for the dial instrument, which has enabled the method to concentrate the processing on the surface of the dial instrument.

As a summary of the comparison shown in the Table 2, the proposed method has achieved the pointer tracking and digitization of the dial instrument surface without using the neural network. Therefore, the proposed method satisfied the real time constraints in terms of

memory and time consuming. The proposed method can recover the failure detection once it has been generated through keep a track for the coordinates of pointer and fix the location of the FULL and EMPTY reference points. Moreover, the proposed method has introduced and improved the idea of the black-white mask not only for processing the surface of dial instrument but also extracting the region of interest from the complex surrounding environment.

5. CONCLUSIONS

This paper presented a proposed method not only for localizing the main reference in the dial instrument, but also for tracking and monitoring the pointer's move. The main references of the dial instrument have been defined by FULL and EMPTY area which have been designed for Oxygen pressure. Determining the reference's centre point enables the proposed method to digitize the pointer's moves while the instrument dial is running. Therefore, the proposed method can use this digitization to define in more details the oxygen pressure. Once the coordinate of the pointer has been moved toward the EMPTY area, an emergency alert has been triggered for administrator. The experimental results demonstrate the effectiveness of the proposed method, with improving the performance of the pointer tracking compared with the Hough Transform method. The average tracking time is of approximately 0.37 s without code optimization which ensures the real time requirements. Moreover, the proposed method can be adapted in advance to different shapes of the instrument dial used in industry environments. The scalability highlighted by the proposed method can improve the monitoring task of such instruments not only in the public hospitals but also in across various industrial contexts. The performance of the proposed method has varied from 86% to 100% and it granted a recovery mechanism for the detection and tracking failure by keeping a track for the main reference point on the surface of the dial instrument. Furthermore, the proposed method will be developed to estimate the running status of the dial instrument while the pointer is moving toward FULL or EMPTY reference point.

REFERENCES

[1] T. Wang, L. Shao, X. Chen, H. Liu, Z. Tan, "A method for locating reading area of digital instrument based on color characteristics," IEEE International Conference on Mechatronics and Automation, 2018, doi: 10.1109/ICMA.2018.8484547.

[2] W. Xiaoyuan, W. Jianping, W. Hongfei, "Research on intelligent and digital recognition system and character recognition of electrical instruments," IEEE International Conference on Mechatronics and Automation, 2018, doi: 10.1109/ICMA.2018.8484460.

[3] C. Wang, Y. Fang, L. Jia, "The comparison of canny and structured forests edge detection application in precision identification of pointer instrument," Chinese Control and Decision Conference, 2018, doi: 10.1109/CCDC.2018.8408247.

[4] C. Dai, Y. Gan, L. Zhuo, X. Hu, Y. Wang, Y. Liao, "Intelligent ammeter reading recognition method based on deep learning," IEEE 8th Joint International Information Technology and Artificial Intelligence Conference, 2019, doi: 10.1109/ITAIC.2019.8785764.

[5] K. Cheng, Y. Zhang, H. Zhang, J. Huang, "Research on image processing technology based on analog head reading," Chinese Control And Decision Conference, 2019, doi: 10.1109/CCDC.2019.8833420.

[6] H. Xu, A. Xiong, "Research on machine vision-based reading method for pointer meters," Chinese Control Conference, 2019, doi: 10.23919/ChiCC.2019.8866223.

[7] G. Li, B. Tang, B. Li, X. Luo, Y. Liang, "Image recognition system of pointer meter in substation," IEEE 22nd International Conference on High Performance Computing and Communications, 2020, doi: 10.1109/HPCC-SmartCity-DSS50907.2020.00160.

[8] L. Meng, J. Cheng, "Research on the visual recognition method of pointer water meter reading," IEEE 5th Advanced Information Technology, Electronic and Automation Control Conference, 2021, doi: 10.1109/IAEAC50856.2021.9390735.

[9] Z. Hou, H. Ouyang, X. Hu, "Tilt correction method of pointer instrument," China Automation Congress, 2021, doi: 10.1109/CAC53003.2021.9727588.

[10] G. Lu, Z. Tong, J. Wang, L. Gao, "Intelligent recognition method of indication of substation pointer instrument based on deformable convolution neural network," 4th International Academic Exchange Conference on Science and Technology Innovation, 2022, doi: 10.1109/IAECST57965.2022.10062024.

[11] X. Zhang, S. He, "Application research of pointer instrument panel extraction algorithm based on deep learning," 8th International Conference on Intelligent Computing and Signal Processing, 2023, doi: 10.1109/ICSP58490.2023.10248850.

[12] N. Samet, S. Hicsonmez, E. Akbas, "HoughNet: integrating near and long-range evidence for visual detection", IEEE Transactions on Pattern Analysis and Machine Intelligence, vol. 45, no. 4, pp. 4667–4681, 2023, doi: 10.1109/TPAMI.2022.3200413.

[13] E. Minakov, A. Meshkov, E. Meshkova, "Increasing the detection probability of objects by modified hough transform in radioelectronic surveillance systems," IEEE Conference of Russian Young Researchers in Electrical and Electronic Engineering, 2020, doi: 10.1109/EIConRus49466.2020.9039376.

[14] M. Andreeva, M. Zvezdochkin, "Application of morphological operations and hough transform for recognizing objects in an image when high intensity glare occurs," Intelligent Technologies and Electronic Devices in Vehicle and Road Transport Complex, 2023.

[15] A. Akmakchi, M. Çevik, "Geometric analysis of brain pathology using MRI for TUMOR diagnosis," International Symposium on Multidisciplinary Studies and Innovative Technologies, 2022, doi: 10.1109/ISMSIT56059.2022.9932707.

[16] M. K, A. B, R. Balaji, D. T, "Analysis of face feature recognition using MATLAB," Third International Conference on Artificial Intelligence and Smart Energy, 2023, doi: 10.1109/ICAIS56108.2023.10073828.

[17] Z. Li, S. Lou, "An extracting and labeling algorithm for connected components in images," International Conference on Artificial Intelligence, Big Data and Algorithms (CAIBDA), 2021, doi: 10.1109/CAIBDA53561.2021.00051.

[18] W. Lee, S. Allegretti, F. Bolelli, C. Grana, "Fast run-based connected components labeling for bitonal images," 10th International Conference on Informatics, Electronics & Vision, 2021, doi: 10.1109/ICIEVicIVPR52578.2021.9564149.

[19] X. Zhao, Y. Chao, H. Zhang, B. Yao, L. He, "An efficient connected-component labeling algorithm for 3-d binary images," IEEE Open Journal of the Computer Society, vol. 4, pp. 1–12, 2023, doi: 10.1109/OJCS.2022.3233088.

[20] C. Morris, R. Stark, Fundamentals of Calculus, Hoboken, New Jersey: Wiley, 2015.

[21] H. Li, D. Xiong, Y. Wang, X. Ma, Q. Zhu, "Pixelation algorithm for computing the intersection of connected graphs in intelligent damage recognition," 5th International Conference on Vision, Image and Signal Processing, 2021, doi: 10.1109/ICVISP54630.2021.00063.

[22] A. Posamentier, C. LeTourneau, E. Quinn, *Fundamentals of Algebra: Sourcebook, Course 1*, Sadlier-Oxford, 2009.

[23] *Four-quadrant inverse tangent - MATLAB atan2*, 2023, https://www.mathworks.com/help/matlab/ref/atan2.html.